Zhengyu Liu
Department of Atmospheric and Oceanic Sciences
University of Wisconsin-Madison
Tel: 608/262-0777, Fax: 608/262-0166, Email: zliu3@wisc.edu

Abstract

One of the most important validations for a state-of-art Earth System Model (ESM) with respect to climate changes is the simulation of the climate evolution and abrupt climate change events in the Earth's history of the last 21,000 years. However, one great challenge for model validation is that ESMs usually do not directly simulate geochemical variables that can be compared directly with past proxy records. In this proposal, we have met this challenge by developing the simulation capability of major isotopes in a state-of-art ESM, the Community Earth System Model (CESM), enabling us to make direct model-data comparison by comparing the model directly against proxy climate records. Our isotope-enabled ESM incorporates the capability of simulating key isotopes and geotracers, notably $\delta^{18}O$, δD, $\delta^{14}C$, and $\delta^{13}C$, Nd and Pa/Th. The isotope-enabled ESM have been used to perform some simulations for the last 21000 years. The direct comparison of these simulations with proxy records has shed light on the mechanisms of important climate change events.

Final Technical Report

We have made significant landmarks in our proposed work in the last 5 years (3 years plus 2 years of no cost extension). We have developed the simulation capability of the major isotopes in CESM. In particular, we have completed the implementation of the stable water isotopes ($\delta^{18}O$, δD) into the components for the atmosphere, ocean (Zhang et al., 2016), land surface, runoff transport, sea ice, and coupler. In addition, the carbon isotopes (abiotic and biotic radiocarbon, $\delta^{13}C$) have been implemented into the CESM ocean and land models, and long spinup simulations have been completed (Jahn et al., 2015). Furthermore, we have added abiotic and biotic Neodymium to the CESM ocean model as two tracers of ocean circulation (Gu et al., 2016), which will be compared with proxy data. Fully-coupled simulations with water isotope capability are currently being run for the preindustrial and the Last Glacial Maximum. We have secured 20 million core-hours on the NWSC Yellowstone supercomputer for 12 months in the last year and this year. Together with some CESM Paleoclimate Working Group CSL Yellowstone core hours, we are guaranteed sufficient computing for the spin-up experiments and deglaciation simulations for 21 to 15ka.
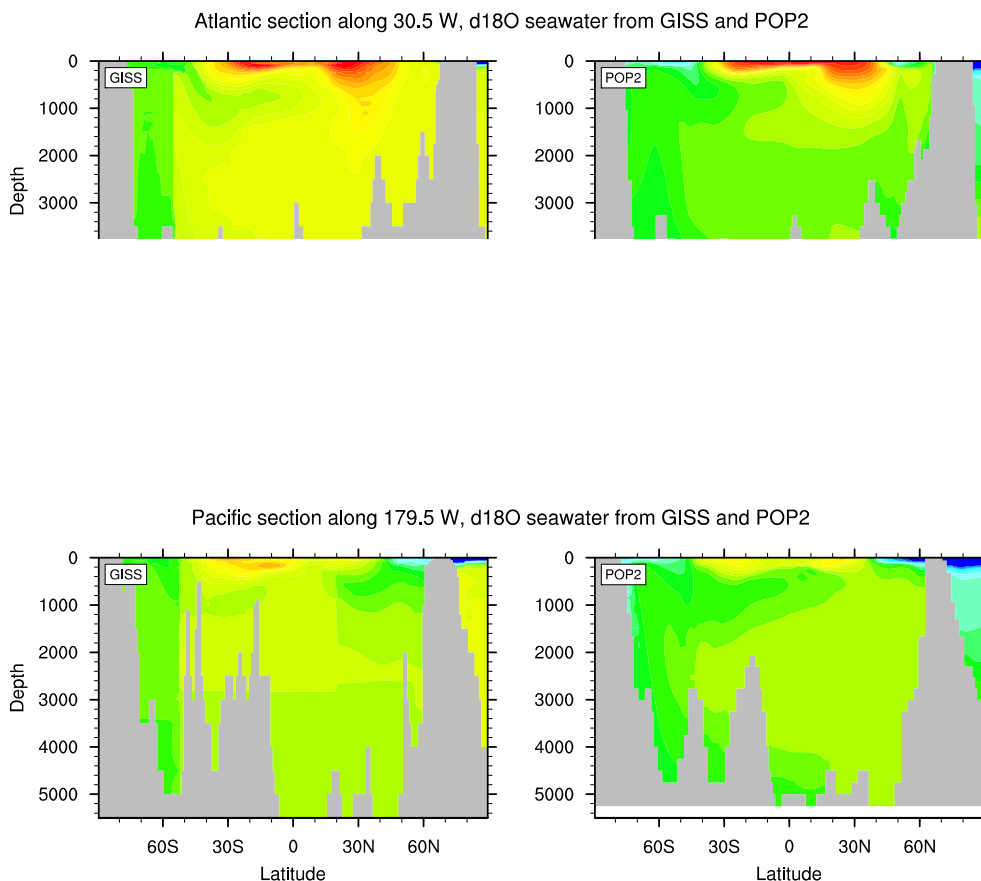
I: Implementation of stable water isotopes [wiso]

The development of wiso-CESM1 has been completed. The $\delta^{18}O$ and δD have been implemented onto the CESM ocean component POP2 (Zhang et al., 2016). The ocean water isotope tracer implementation was tested in stand-alone POP2 3-degree ocean-only simulations forced with CORE2 Normal Year fields and observationally-based monthly mean fields of $\delta^{18}O$ and δD in precipitation based on the Global Network in Precipitation (GNIP) records. Compared to the annual mean gridded NASA-GISS $\delta^{18}O$ database, which uses regressions with other tracers to fill in sparse areas, after 500 years of integration the $\delta^{18}O$ field in the climatologically-forced isotopically-enabled nominally 3-degree POP2 configuration is reasonable as shown in Fig. 1, considering the biases that can be directly related to biases in the simulated circulation of the 3-degree POP2 model. In particular, the simulation shows a much more 'depleted' water column in the Southern Hemisphere (SH) and in deep water originating in the SH, as compared to the database, where the 3-degree POP2 model over produces Bottom Water, and the deep ocean in the North Atlantic is too depleted where the Atlantic Meridional Overturning (AMOC) is too   nd to biases in
the i   erved fields,
espe   isotopic values
in ru   cal
prec   local delta
value

Atlantic section along 30.5 W, d18O seawater from GISS and POP2

Pacific section along 179.5 W, d18O seawater from GISS and POP2

Figure 1: Pacific and Atlantic cross sections of the $\delta^{18}Ow$ in the 1x1° gridded NASA-GISS Global Seawater Oxygen-18 Database (Legrande and Schmidt, 2006) and simulated in POP2 after 200 years starting from a zero $\delta^{18}O$ value with monthly mean climatological forcing.

In collaboration with David Noone at Oregon State University (OSU) and his graduate students at the University of Colorado-Boulder (CU) [under separate grant], $\delta^{18}O$ and δD have been implemented into the CESM atmosphere component CAM5.3. A major accomplishment was the completion of the water tracer framework needed to properly manage water isotopologues in the model physics routines. This framework also allows for water tagging experiments, which is when a water tracer is added to the model that behaves just like regular water, but is constrained in such a way as to provide information on the sources and sinks of water in the simulated climate. For example, one can create a water tracer that only evaporates over a single grid box, which can then be used to quantify the amount of local moisture recycling that occurs in the grid box. This technique can ultimately help expand the scientific capabilities of iCESM, particularly for studies in hydrology.

In terms of stable water isotopologues, the cloud physics and convective parameterization schemes in CAM5.3 have been enhanced to allow for isotopic equilibration and fractionation. These new isotopic processes, combined with the already existing fractionation produced by evaporation from the ocean, results in a more accurate simulation of isotopic ratios in atmospheric water vapor, as can be seen in Fig. 2.
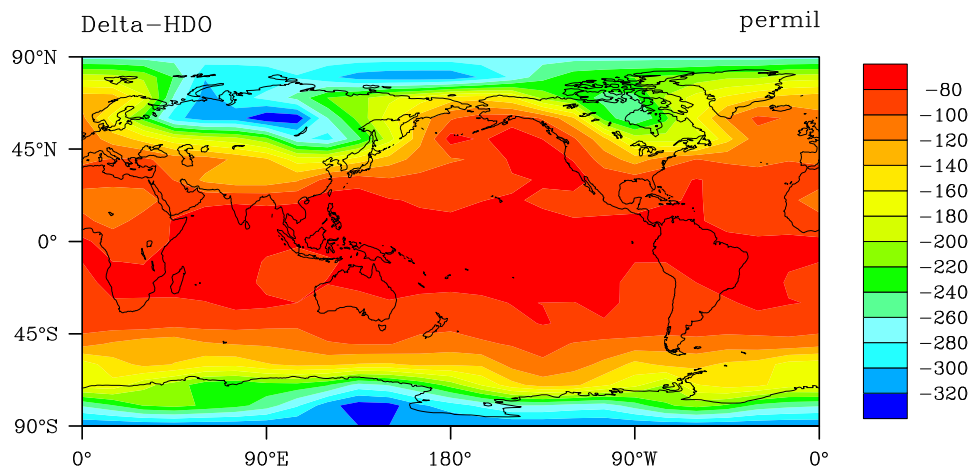
Average vapor delta-D at ~760 mb after six months

Figure 2: A map of water vapor δD at approximately 760 mb, as simulated by CAM5 with isotope-enabled cloud physics schemes and isotopic fractionation produced by oceanic evaporation.

Comparing with previous versions, more complete new processes of the isotopic hydrological cycle have been incorporated into the land component CLM4, the runoff transport model RTM, and the sea ice component CICE4 of CESM. In wiso-CLM, progress by OSU/CU collaborators includes a new cellulose model dealing with isotopic leaf water and an updated canopy module simulating the Peclet effect. In wiso-CICE, the isotopic reference vapor mixing ratio and evaporation flux, which are required by the isotope-enabled atmosphere model, are now calculated and delivered to the atmosphere. Additionally, a new sea ice growth rate-dependent fractionation process has been incorporated into the model, which will change the isotopic water

flux to the ocean. After including more complete processes, the wiso-CICE model has been thoroughly tested by conducting the "constant-ratio test". The idea is that we initialize and force the isotopic water in the same way as regular water (with fractionations turned off), and we expect the solutions for isotopic water are exactly the same as regular water. This helps us to make sure that the isotopic hydrological cycle has been simulated as accurate as the regular hydrological cycle in the model.

After validating each component model, the water isotope-enabled components (atmosphere, land, ocean, sea ice, runoff) have been coupled together. Efforts have been made to verify that state variables and fluxes are passed correctly across different model components. A fully coupled isotope-enabled simulation for preindustrial conditions has been performed. Our preliminary analysis of the coupled model shows it is able to reproduce the general patterns of the available observations very well, including the main features in observed $\delta^{18}O$ in precipitation, surface ocean and deep ocean (Fig. 3). Our fully coupled model simulation shows the importance of including the full isotopic hydrologic cycle including transport by rivers and sea ice processes (Fig. 4). Without including these processes, the high latitude ocean is insufficiently depleted compared to observations, especially in the Arctic basin. Currently, software engineers at NCAR are working closely with the model developers to incorporate the new isotope code within the CESM development trunk. We are also currently running the wiso-TRACE21 experiment for the Last Glacial Maximum.
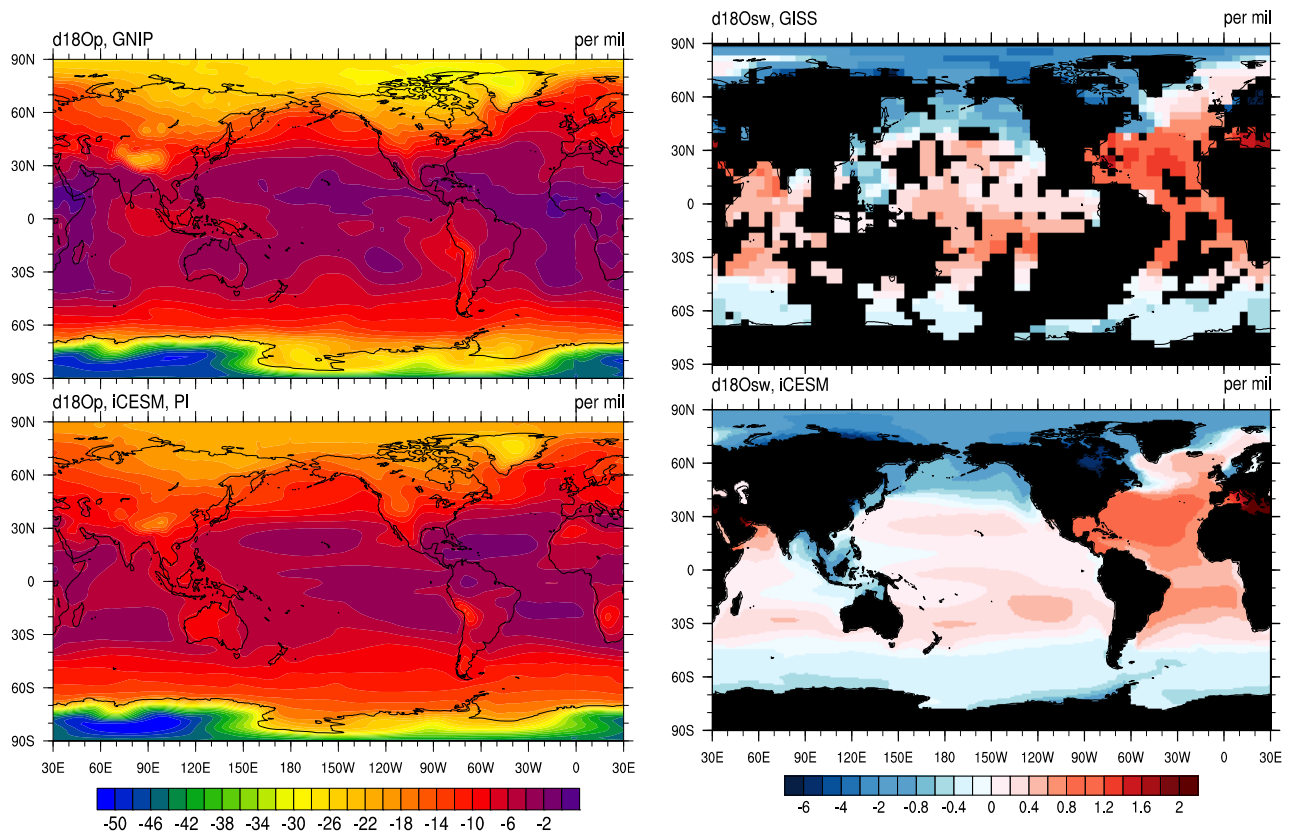

Figure 3: $\delta^{18}O$ of precipitation (left) and surface seawater (right) simulated in wiso-CESM as compared to observational datasets.

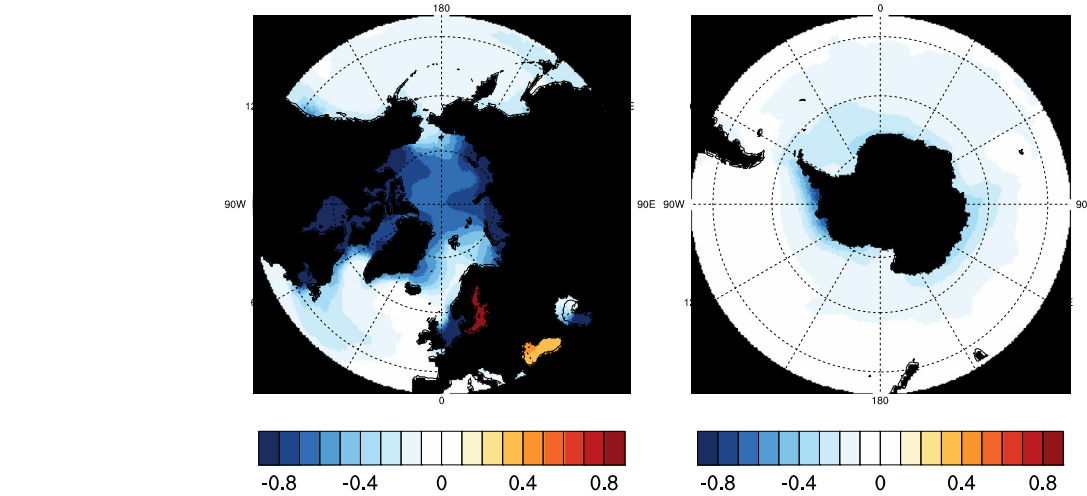Figure 4: Difference in $\delta^{18}O$ (per mil) between the fully coupled wiso-CESM (fig. 3) simulation, including the isotopic CLM, CICE and RTM components, and an earlier version with just the isotopic enabled CAM, and POP models coupled.

II: Implementation of carbon isotopes [ciso]

An abiotic formulation of radiocarbon (^{14}C) has been added to the CESM ocean component POP2, in collaboration with Keith Lindsay (NCAR) (Jahn et al., 2015). This implementation was done following the OCMIP2 (ocean Carbon Model Intercomparison Project phase 2) protocol, with some improvements. The improvements are that we use the sea ice fraction from the sea ice model (either the data model or the CICE model) as well as wind forcing from the atmosphere model (either the data model or CAM) to calculate the piston velocity for the gas exchange calculation. This means that we can solve the fully-coupled radiocarbon problem rather than the ocean-only problem. As it is an abiotic radiocarbon implementation, the code can be run without the ecosystem model, which limits the increase in the computational cost to 20% compared to a normal POP2 simulation, compared to a 200% increase in computational cost for the use of an active ecosystem mode.

The radiocarbon code was tested extensively for the ocean-only and ocean-ice configuration in the 3-degree model configuration. This testing included a 10,000-year long spin-up under equilibrium pre-industrial conditions, which was needed to bring the radiocarbon simulation into equilibrium. Subsequently we performed transient simulations for 1765 to 2007, simulating the natural and bomb radiocarbon in the ocean. In these simulations, atmospheric radiocarbon and CO_2 concentrations were prescribed based on observational datasets. Furthermore, the radiocarbon code was also tested for functionality in the fully coupled model, where the CO2 concentration used in the radiocarbon code is the same as the CO_2 concentration used in other components (i.e., the atmosphere for radiative transfer calculations, the land and ocean ecosystem models for biological productivity, etc).

Compared to cruise data compiled by Schmittner and the gridded GLODAP radiocarbon data, we find a reasonable agreement to the model results (Fig. 5), taking into account the model biases in the 3-degree model, which include too much deep water formation in the Southern Ocean, too weak deep water formation in the North Atlantic, and too weak circulation in the deep Pacific. Compared to radiocarbon data from coral records, we find that the model also reproduces the observed bomb-spike reasonably well, given the coarse model resolution. We expect that using the 1-degree model will yield much better results, given the generally better climate simulation in the 1-degree ocean model. Due to the biases in the 3-degree ocean model,

we plan to use the 1-degree ocean model coupled to a 2-degree atmosphere model for the iTRACE simulations. In addition, the fast spin-up technique developed by Keith Lindsay, which makes use of a preconditioned Newton-Krylov solver to generate equilibrium solutions for the abiotic radiocarbon, will be used to generate initial conditions for the abiotic carbon tracers for the iTRACE simulations, which would otherwise take over 5000 model years to spin up.
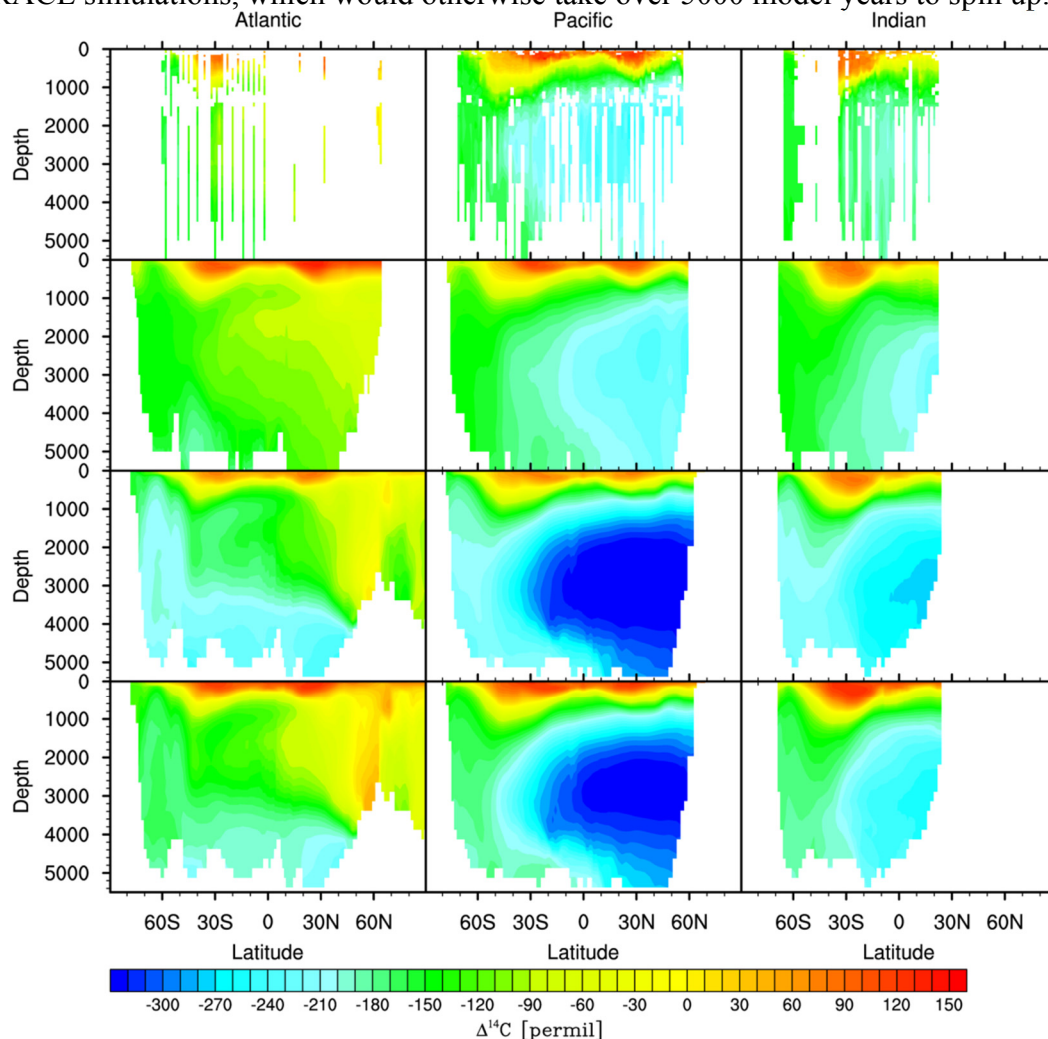

Figure 5. Zonal averages of total $\Delta^{14}C$ for the Atlantic, Pacific, and Indian oceans for the 1990s, from cruise data compiled by Schmittner et al. (Biogeosciences, 2013) (top row), the gridded GLODAP data (Key et al., Global Biogeochem. Cy., 2004) (second row), the ^{14}C from the biotic model (third row), and the abiotic model (bottom row). Note that due to the sparse observational data, the zonal average from the cruise data in the top row is more of a zonal composite than a zonal average.

After the addition of the abiotic radiocarbon module, an additional module for biotic ^{13}C and ^{14}C was added (Jahn et al., 2015). The ^{13}C implementation was based on existing code from ETH in POP1.4. It requires the ecosystem model to run, and is therefore more expensive than the abiotic radiocarbon code. Overall, the computational expense of the biotic carbon isotope module is 4 times the expense of the ocean-only model, and 1.4 times the expense of running the ocean model with the ecosystem model. The implementation of the biotic carbon isotopes required significant code modifications to follow the ocean model code development guidelines and to make it easier to add additional biotic isotopes and tracers that require the ecosystem model (like Pa/Th).

The carbon isotope module calculates the carbon isotopic fractionation during gas exchange, photosynthesis, and calcium carbonate formation, while any subsequent biological process such as remineralization as well as any external inputs are assumed to occur without fractionation. Given the uncertainty associated with the biological fractionation during photosynthesis, we implemented and tested three parameterizations of different complexity (Fig. 6). We completed a 6000 year spin-up with the biotic carbon isotope tracers, followed by a simulation for 1765 to 2007. Compared to present-day observations, the model is able to simulate the oceanic ^{14}C bomb uptake and the [13]C Suess effect reasonably well compared to observations and other model studies. At the same time, the carbon isotopes reveal biases in the physical model, for example, too sluggish ventilation of the deep Pacific Ocean (Fig. 5).
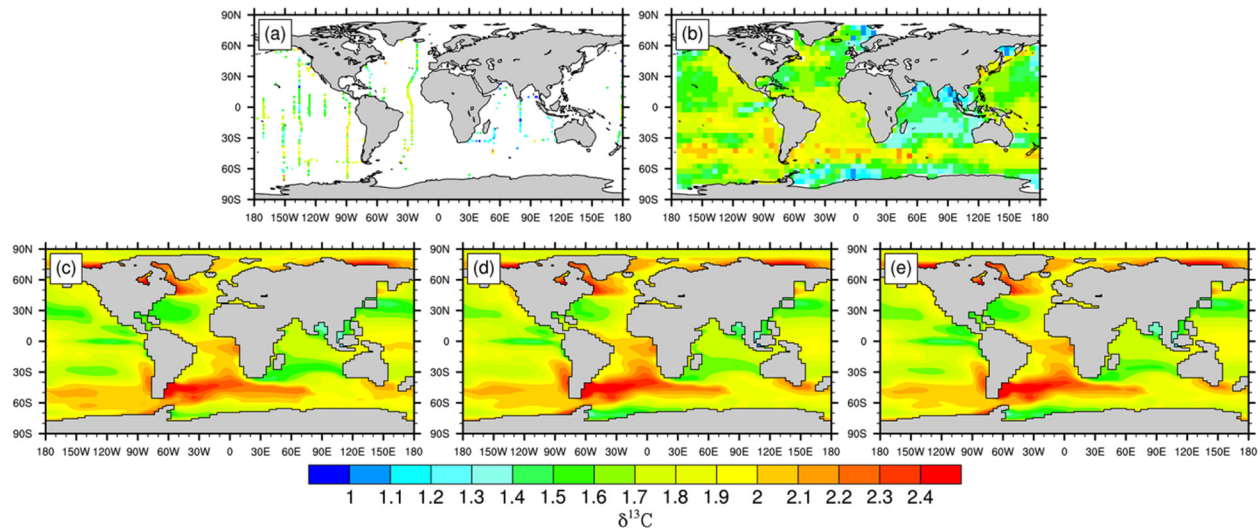

Figure 6. Surface values of $\delta^{13}C$ for the 1990s from (a) cruise data compiled by Schmittner et al., (b) 5° extrapolated gridded data from Gruber and Keeling (1999) and Gruber and Keeling (2001), and (c–e) the biotic model, using the biological fractionation from (c) Rau et al. (Nature, 1989), (d) Laws et al. (Geochem. Cosmochim. Ac.,1995), and (e) Keller and Morel (Mar. Ecol.-Prog.Ser., 1999).

Building upon earlier implementations for the ^{13}C and ^{14}C tracers in CLM, A. Bozbiyik (doctoral student, U. Bern) has advanced significant progress in extending the implementation of the ^{13}C and ^{14}C isotope tracers in CLM4.5. This implementation is compatible with the overall development of the soil code in the latest development versions of CLM to be included in future CESM releases. CLM4.5 includes a fully prognostic representation of the fluxes, storage, and isotopic discrimination of the carbon isotopes ^{13}C and [14]C. The new implementation of the C isotopes capability takes advantage of the CLM hierarchical data structures, replicating the carbon state and flux variable structures at the column and PFT level to track total carbon and both C isotopes separately. To test the new implementation, the carbon-isotope enabled version of the CLM is run in a stand-alone configuration, forced with Qian et al. Climatology over the period 1948-1972. To fill the ^{13}C pools, an initial $\delta^{13}C$ value of -13 per mil is set for C-4 plants and -28 per mil for C-3 plants. For column level pools, such as soil pools, a value of -28 per mil is set because the slow decomposing high northern latitudes are dominated by C-3 plants. The model is run for 700 years in Accelerated Decomposition mode, then for another 180 years in a non-accelerated mode. Fig. 7 shows that the model manages to capture the isotopic differences between C-3 and C-4 plants, which have different photosynthetic pathways and so discriminate

against ^{13}C by different amounts with C-3 plants having a much larger discrimination (more negative values) than C-4 plants.
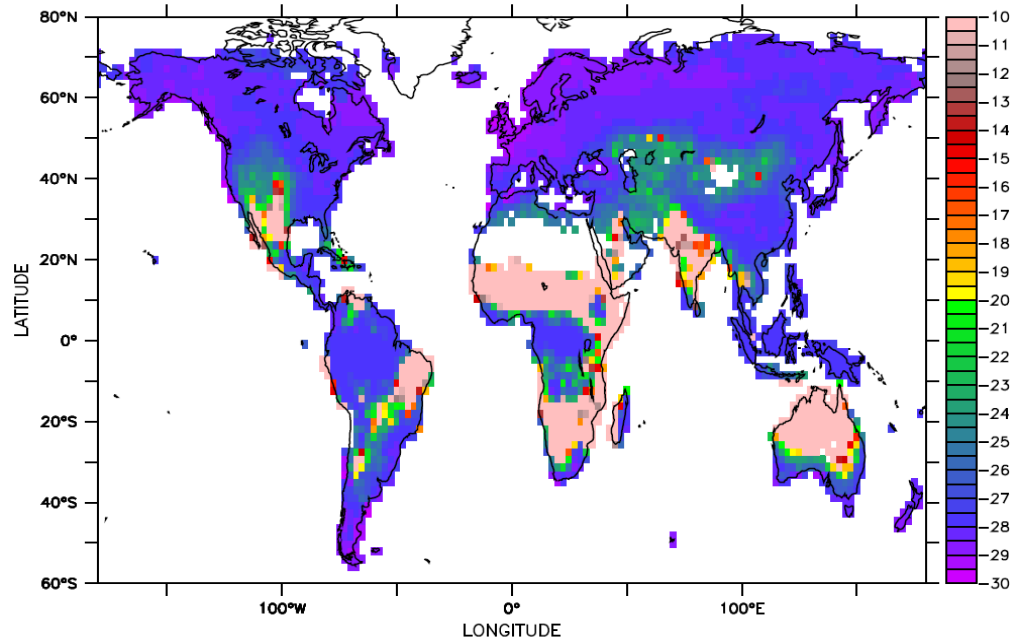

Figure 7: Global δ^{13}C of the Total Vegetation at the end of the spin-up. This map shows a 25-year average over the end of the previous slide. The time frame to be averaged is selected to reflect the repetition loop of the applied climatology fields.

III: Implementation of Neodymium tracer in POP

We have also implemented both an abiotic and biotic Neodymium tracers in the CESM ocean component POP2 (Gu et al., 2016). This implementation follows the scheme described in Rempfer et al. (Geochem. Cosmochim. Ac., 2011). Abiotic eNd can be used to trace water mass mixing because of the inter basin gradient of eNd values. For intermediate water cores in the Atlantic, the sign and magnitude of the simulated deglacial changes are comparable to reconstructions. For deep ocean cores, the sign of the simulated deglacial changes is consistent with reconstructions but with smaller magnitude. For a north-south time slice in the Atlantic, the deep ocean shows an increase of eNd during Heinrich event 1 (H1, 16 ka) and a decrease of eNd at the Bolling-Allerod (14.35 ka), suggesting a north-sourced versus south-sourced water mass change (Fig. 8). A fully biotic version is also implemented, which is coupled with the ecosystem model through the production rate. Several sets of sensitivity experiments have been performed for different sedimentation rate and total source magnitude and the optimal parameter set has been selected, comparable with Rempfer et al. in the Bern Ocean model. In addition Pa/ and Th have also been implemented, again coupled with the ecosystem and is currently under testing.
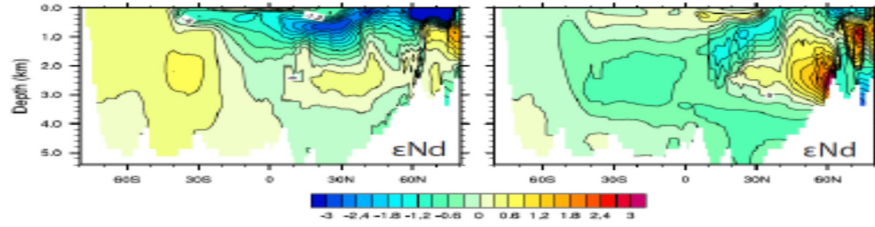
Figure 8: The difference of the simulated abiotic eNd in the ocean wiso-TRACE21 simulation. The left column shows the difference between 16ka and 19ka, representing the H1 event, and the right column shows the difference between 14.35ka and 19ka, representing the BA transition from the LGM.

IV. Uncoupled simulations

In preparation for the upcoming wiso-TRACE21 simulation, we initiated a pilot study to study the $\delta^{18}O$ evolution in the ocean using the water isotope ocean component of the upcoming wiso-CESM1. This ocean wiso-TRACE is forced by the physical fields from our previous TRACE21 simulation as well as a series of snapshot experiments in wiso-CAM3. It has not been a trivial task to reproduce the TRACE21 ocean evolution using its surface fields, because the model output only retains monthly mean values and the present ocean model is in POP2, instead of POP1 in TRACE21 (Zhang et al., 2016). There is so far no publication on a successful scheme that can reproduce the ocean circulation in a fully coupled climate model using its ocean component and monthly model output. After numerous tests in the past year, we have succeeded in a hybrid surface flux scheme that uses a combination of both surface flux and restoring. This can be seen in the similarity of the two simulations in both the strengths of the AMOC and the Antarctic Bottom Water (AABW) (Fig.9). The similar physical circulation between POP2 and TRACE21 ensures the simulated isotopes in POP2 are representative of those in TRACE21 (were those tracers implemented).
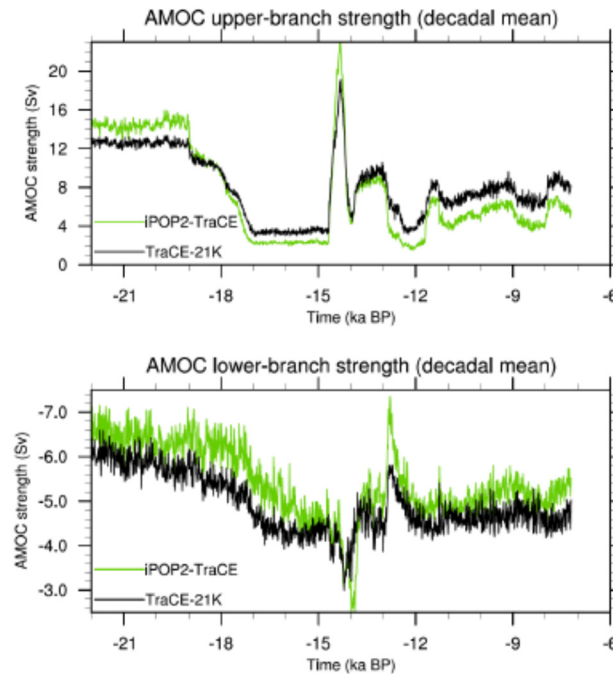
Figure 9: Time evolution of the strengths of (top) the AMOC and (bottom) AABW in the POP2 (green) and TRACE (black). The simulation has been integrated so far to ~7ka and will be continued to the present.

V: TraCE analysis and isotope sensitivity experiments

In preparation for and for comparison to the iTRACE21 simulations to be preformed with the isotope-enabled CESM, we have completed additional analysis of the TRACE21 full-forcing and single-forcing simulations. The complex simulated behavior of ENSO during the deglaciation is shown to be a result of abrupt response to the meltwater and ice sheet forcings and more gradual changes associated with orbital and CO_2 forcings (Liu et al., 2014a, Lu et al., 2015). The abrupt onset of the African Humid Period in southeastern equatorial and northern Africa is shown to be coincident with the reestablishment of the AMOC with the termination of the Heinrich-1 meltwater event, while the subsequent coherent wetter conditions in both regions is a response to the increasing greenhouse gas concentrations (Otto-Bliesner et al., 2014). At high latitudes, TRACE21 indicates a linear weakening of the AMOC in response to the receding glacial ice sheets (Zhu et al., 2014). Also, the response of the AMOC to green house gases is found to be dependent on background states and different timescales (Zhu et al., 2015). Atmospheric isotope snapshot studies using output from the TRACE21 simulation have also been analyzed to better understand the interpretation of the Greenland ice core records (Liu et al., 2012) and Chinese cave speleothem records (Liu et al., 2014b; Wen et al., 2016). A recent study further sheds insight onto the temporal slope of the temperature-18O relation in high latitude ice cores (Guan et al., 2016), in which a semi-theoretical equation is derived for the relation between the temporal slope and spatial slope, representing a significant step in understanding the water isotope and its climate representation.

VI: Collaborations

This work was designed as an intensive collaboration among UW-Madison, NCAR and other institutions, especially CU and Univ. Bern, which has proven to be critical for the success of the project. This collaboration was further expanded to a new and fruitful collaboration with Chinese scientists, Drs. Xinyu Wen, Ge Yu, Yongjin Wang et al., for the understanding of the behavior of water isotope and its relation with Asian monsoon climate evolution during the last deglaciation, which has been a key motivation for implementing water isotope in CESM here. As a result, some international travel expenses are used from this grant.

VII: Future work

We have several major tasks for the future. With our iTRACE21 simulations with water isotopes and radiocarbon, we will revisit as well as continue to expand our model-data comparisons of regional abrupt climate changes and the roles of individual forcing: CO_2, ice sheet, meltwater and orbital forcing. We are also transitioning the water and carbon isotope implementations to the CESM2. Finally, we will use the multi-isotope-enabled (water, carbon 14, carbon 13, Nd, Pa/Th) ocean model: iPOP2, to simulate the oceanic evolution of the last 21,000 years forced by the coupled climate forcing from CESM.

Publications

Gu, S., Z. Liu, J. Zhang, E. Brady, J. Rempfer and F. Joos, 2016: Coherent dynamic response of Antarctic Intermediate Water and Atlantic Meridional Overturning Circulation during deglaciation. *PNAS*, submitted.

Guan, J. Z. Liu, X. Wen, E. Brady, D. Noone, J. Zhu and J. Han, 2016: Understanding temporal slope of temperature-water isotope relation in isoCAM3: the slope equation. *J. Geophys. Res.*, **121**, 10.1002/2016JD024955

Jahn, A., K. Lindsay, X. Giraud, N. Gruber, B. L. Otto-Bliesner, Z. Liu, and E. C. Brady, 2015: Carbon isotopes in the ocean model of the Community Earth System Model (CESM1). *Geosci. Model Dev.*, **8**, 2419-2434.

Liu, Z., A.E. Carlson, F. He, E.C. Brady, B.L. Otto-Bliesner, B.P. Briegleb, M. Wehrenberg, P.U. Clark, S. Wu, J. Cheng, J. Zhang, D. Noone and J. Zhu, 2012: The Younger Dryas cooling and the Greenland response to CO_2. *PNAS*, **109**, 11101-11104. doi/10.1073/pnas.1202183109.

Liu Z., Z. Lu, X. Wen, B.L. Otto-Bliesner, A. Timmermann, K.M Cobb, 2014a: Evolution and forcing mechanism of El Nino over the past 21,000 years. *Nature*, **515**, 550-553

Liu, Z., X. Wen, E.C. Brady, B. Otto-Bliesner, G. Yu, H. Lu, H. Cheng, Y. Wang, W. Zheng, Y. Ding, R.L. Edwards, J. Cheng, W. Liu and H. Yang, 2014b: Chinese cave records and the East Asian Summer Monsoon. *Quat. Sci. Rev.*, **83**, 115–128.

Lu, Z., Z. Liu, J. Zhu, 2015: Abrupt intensification of ENSO forced by deglacial ice sheet retreat in CCSM3. *Clim. Dyn.*, DOI 10.1007/s00382-015-2681-3

Otto-Bliesner, B.L., J.M. Russell, P.U. Clark, Z. Liu, J.T. Overpeck, B. Konecky, P. deMenocal, S.E. Nicholson, F. He and Z. Lu, 2014: Coherent changes of southeastern equatorial and northern African rainfall during the last deglaciation. *Science*, **346**, 1223-1227. DOI: 10.1126/science.1259531

Wen Xinyu, Z. Liu, Zhongxiao Chen, Esther Brady, David Noone, Qingzhao Zhu, Jian Guan, 2016: Modeling Precipitation d[18]O Variability in East Asia since the Last Glacial Maximum: Temperature and Amount Effects across Different Time Scales. *Climate of Past,* discussion. doi:10.5194/cp-2016-2

Zhang, J., Z. Liu, E. Brady, S. Gu, K. Lindsay, J. Gottschalk and D. Oppo, 2015: Dynamic warming of Atlantic abyssal water mass during deglacition. *PNAS*, submitted.

Zhu J., Z. Liu, J. Zhang, W. Liu, 2015: AMOC response to global warming: Dependence on the background climate and response timescale. *Clim. Dyn.*, **44**, 3449-3468.

Zhu J., Z. Liu, X. Zhang, I. Eisenman and W. Liu, 2014: Transient weakening of the AMOC to receding glacial ice sheets in CCSM3 and its physical mechanism. *Geophys. Res. Lett.*, **41**, 6252–6258, doi:10.1002/2014GL060891.